


## High-Order Exceptional Points in Pseudo-Hermitian Radio-Frequency Circuits

Ke Yin<sup>1</sup>, Xianglin Hao<sup>1</sup>, Yuangen Huang<sup>1</sup>, Jianlong Zou<sup>1</sup>, Xikui Ma, and Tianyu Dong<sup>1\*</sup>

*School of Electrical Engineering, Xi'an Jiaotong University, Xi'an, 710049, China*

 (Received 18 April 2023; revised 11 June 2023; accepted 1 August 2023; published 15 August 2023)

Exceptional points (EPs) in non-Hermitian systems have been widely investigated due to their increased sensitivity in comparison with standard systems. In this Letter, we report the observation of higher-order pseudo-Hermitian degeneracies in an electronic platform comprising three inductively coupled gain-loss  $LC$  resonators. Theoretical analysis demonstrates that the proposed system can realize third-order EPs with asymmetric coupling between adjacent inductors and an arbitrary scaling factor between two loss resonators. When capacitive perturbation is introduced on the middle resonator, the perturbed eigenfrequencies follow a cube-root dependence on the perturbation parameter; in this case, the sensitivity is significantly greater than that of conventional wireless readout methods. Our work enriches the explorations of higher-order EPs on electronic platforms and provides a new degree of design freedom for the non-Hermitian-EP-enhanced wireless sensing system.

DOI: [10.1103/PhysRevApplied.20.L021003](https://doi.org/10.1103/PhysRevApplied.20.L021003)

An exceptional point (EP) is a singularity in the parameter space of the system where the eigenvalues and their corresponding eigenvectors coalesce [1]. In recent decades, the characteristics of EPs in non-Hermitian systems, especially parity-time- ( $PT$ ) symmetric systems, have been intensively studied in a variety of physical settings, including optical waveguides [2,3], microresonators [4], cavity magnon-polaritons [5], and coupled inductor-capacitor ( $LC$ ) resonators [6–13]. The phase-transition properties at EPs are commonly associated with intriguing phenomena, such as asymmetric mode switching [3], single-mode lasing [14,15], and increased sensitivity to external perturbations [8,16]. Increased-sensitivity optical sensing systems based on second-order EPs in non-Hermitian systems were proposed for nanoparticle detection by Wiersig [17]. Later, higher-order EPs (HOEPs) with even higher sensitivities were proposed and experimentally validated [16]. By borrowing the concept from the pseudo-Hermitian condition for realizing non-Hermitian systems with real eigenvalues [18,19], some researchers propose that pseudo-Hermitian systems without  $PT$  symmetry can also exhibit HOEPs [20]. Until now, the properties of pseudo-Hermitian EPs have been mostly investigated in optical systems and their study has yet to be extended to radio-frequency electronic circuits. In our work, it is demonstrated that coupled  $LC$  resonators with pseudo-Hermiticity operated at HOEPs can realize wireless sensing systems with increased sensitivity.

The idea of wirelessly monitoring physiological parameters through inductively interrogating  $LC$  microresonators

was proposed by Collins [21] to measure intraocular pressure. The conventional readout method involves inductively coupling the passive microsensor to a readout antenna, which is connected to a vector network analyzer (VNA) for reflection measurement. The measured parameter induces the resonant-frequency change of the  $LC$  microsensor and successively introduces a dip frequency shift of the reflection spectra. During the last few decades, the microsensor design and manufacturing process itself have been greatly improved with the development of MEMS technology [22–24]. However, fewer efforts have been made to improve the readout performance, i.e., resolution and sensitivity, of the sensing system, which has hindered the real-life application of the passive  $LC$  sensor. Recently, it was proposed that a  $PT$ -symmetric wireless sensing system can increase the resolution of the readout spectrum [25–28]. Furthermore, by use of the eigenvalue bifurcation properties of EPs, the sensitivity of the response to the parameters to be measured can be increased [8–12,29]. For instance, perturbed eigenvalues at a second-order EP (EP2) and a third-order EP (EP3) with increased sensitivity have been observed in a radio-frequency  $PT$ -symmetric system [7,8]. Along different lines, it is proposed that a EP2-locked reader with  $PT$  symmetry can interrogate  $LC$  sensors with sensitivity greater than that of the standard reader [9], which has been extended to the HOEP-locked reader [29]. Furthermore, a  $PT$ -symmetric EP that coincides with a divergent singularity can realize a divergent EP with tremendously large eigenvalue bifurcation, thereby significantly increasing the sensitivity [11,12]. In typical  $PT$ -symmetric systems with EP3 consisting of coupled gain-neutral-loss resonators, the neutral resonator is considered completely lossless. However, this is typically not the case in practical  $LC$  sensors, which

\*Corresponding author. tydong@mail.xjtu.edu.cn

exhibit Ohmic loss due to the high-frequency skin effect of the coils [23,30,31]. Fortunately,  $PT$  symmetry is only a sufficient but unnecessary condition for construction of HOEPs [20]. Instead, the more-general pseudo-Hermitian wireless sensing systems can be designed to exhibit EP3, relaxing the condition of  $PT$  symmetry.

In this Letter, we propose a pseudo-Hermitian wireless sensing system consisting of gain-loss-loss  $LC$  resonators, which can be designed to exhibit EP3. It is shown that the relay resonator with loss results in the adjacent coupling conditions for EP3 to be asymmetric. When capacitive perturbation is introduced on the relay resonator, the perturbed eigenfrequency follows a cube-root dependency on the perturbation parameter, showing much greater sensitivity than the conventional wireless readout method. Differently from the ultrahigh sensitivity of a divergent EP, which relies on both the strong coupling condition and balanced gain and loss [11], the increased sensitivity in our system is due to the cube-root-dependent perturbation behavior of the pseudo-Hermitian EP3. Our work demonstrates that EP-enhanced sensing can be used under asymmetric gain-loss distribution given that the pseudo-Hermitian condition is satisfied, thereby introducing a new degree of design freedom for the HOEP-based wireless sensing system.

A schematic of the proposed pseudo-Hermitian electronic trimer, consisting of three planarly inductively coupled  $RLC$  series resonators is shown in Fig. 1(a). For generality, we first assume all three resonators are lossy,

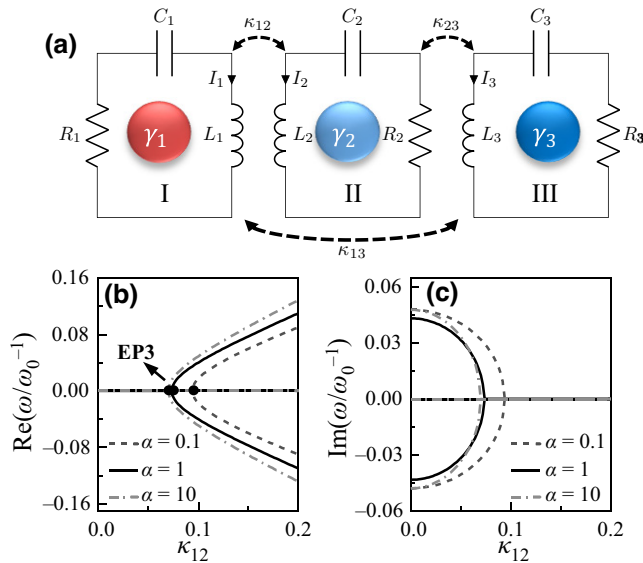


FIG. 1. (a) Illustration and circuit schematic of the pseudo-Hermitian electronic trimer, which is composed of three planarly inductively coupled  $RLC$  resonators. (b) Real part and (c) imaginary part of eigenfrequency evolution as a function of  $\kappa_{12}$  at different scaling factors  $\alpha$  when  $g = 0.1$ ,  $\kappa_{13} = 0$ , and  $\kappa_{23} = (1 + \alpha)^{-3/2}\kappa_{12}$ .

with loss parameter  $\gamma_n$  ( $n = 1, 2, 3$ ). By obtaining the conditions for HOEPs, we can determine the gain and loss parameters

The system equation for the proposed system derived from coupled-mode theory reads  $id\mathbf{I}/dt = \hat{H}_0\mathbf{I}$ , where  $\mathbf{I} = (I_1, I_2, I_3)^T$  is the system variable and

$$\hat{H}_0 = \frac{\omega_0}{2} \begin{pmatrix} 2 - i\gamma_1 & \kappa_{12} & \kappa_{13} \\ \kappa_{12} & 2 - i\gamma_2 & \kappa_{23} \\ \kappa_{13} & \kappa_{23} & 2 - i\gamma_3 \end{pmatrix} \quad (1)$$

is the effective Hamiltonian operator, where  $\omega_0 = 1/\sqrt{L_n C_n}$  denotes the resonant frequency, with  $L_n = L$  and  $C_n = C$  for  $n = 1, 2, 3$ ;  $\gamma_n = R_n\sqrt{C/L}$  is the gain or loss parameter; and  $\kappa_n = M_n/L$  is the inductive-coupling coefficient, where  $M_n$  is the mutual inductance.

After the substitution  $\lambda = \omega/\omega_0 - 1$ , the real and imaginary parts of the characteristic equation  $\det(\hat{H}_0 - \omega\mathbb{I}_3) = 0$ , with  $\mathbb{I}_3$  being a  $3 \times 3$  identity matrix, respectively read

$$\lambda^3 - \frac{1}{4} \sum_{m<n} (\gamma_m \gamma_n + \kappa_{mn}^2) \lambda - \frac{1}{4} \prod_{m<n} \kappa_{mn} = 0, \quad (2a)$$

$$\sum_{m=1}^3 \gamma_m \lambda^2 - \frac{1}{4} \prod_{m=1}^3 \gamma_m \left( 1 + \sum_{m<n} \frac{\kappa_{mn}^2}{\gamma_m \gamma_n} \right) = 0, \quad (2b)$$

where  $m = 1, 2, 3$  and  $n = 1, 2, 3$ . Here  $\omega_0$  is normalized to 1 for concision. With the characteristic equation, we can then determine the conditions for the system to be pseudo-Hermitian as well as the conditions for the emergence of third-order EPs.

To guarantee pseudo-Hermiticity, the Hamiltonian should satisfy  $\det(\hat{H}_0 - \omega\mathbb{I}_3) = \det(\hat{H}_0^* - \omega\mathbb{I}_3)$ , i.e.,  $\text{Im}[\det(\hat{H}_0 - \omega\mathbb{I}_3)] = 0$ , which yields

$$\sum_{m=1}^3 \gamma_m = 0, \quad (3a)$$

$$\prod_{m=1}^3 \gamma_m \left( 1 + \sum_{m<n} \frac{\kappa_{mn}^2}{\gamma_m \gamma_n} \right) = 0. \quad (3b)$$

Here, Eq. (3a) implies that balanced total gain and loss of the system should be satisfied. As can be seen from Eq. (2a), the third-order EP  $\lambda_{\text{EP3}}$  arises when

$$\sum_{m<n} (\gamma_m \gamma_n + \kappa_{mn}^2) = 0, \quad (4a)$$

$$\prod_{m<n} \kappa_{mn} = 0. \quad (4b)$$

Taking into account the structure of the wireless sensing system and using the gain introduced by the VNA, we consider the case where  $\gamma_1 = -g$  and  $\gamma_2 = \alpha\gamma_3$ , i.e., the

first resonator has gain, while the other two resonators are lossy with loss parameters that differ by  $\alpha$ . It should be pointed out here that the gain element is considered linear as opposed to nonlinear and saturable. The latter is typically used in transient  $PT$ -symmetric systems where nonlinear active components are used to construct the gain [9,10,32]. From Eq. (3a),  $\gamma_2$  and  $\gamma_3$  can be derived as  $\gamma_2 = g\alpha/(1+\alpha)$  and  $\gamma_3 = g/(1+\alpha)$ , respectively. Note that when  $\alpha = 0$ , the system is a  $PT$ -symmetric trimer with a neutral relay resonator. By solving Eqs. (3b) and (4), one can determine the coupling coefficients  $\kappa_{12}$ ,  $\kappa_{13}$ , and  $\kappa_{23}$  for a given gain parameter  $g$ . Note that the condition given by Eq. (4b) implies that the third-order EP exists only when one of the coupling coefficients is zero. Specifically, when  $\kappa_{12} = 0$ , the derived coupling coefficients are  $\kappa_{13} = g\sqrt{(1+\alpha)/(1+2\alpha)}$  and  $\kappa_{23} = g\alpha\sqrt{\alpha/(1+2\alpha)}/(1+\alpha)$ , respectively; when  $\kappa_{13} = 0$ , we have  $\kappa_{12} = g\sqrt{(1+\alpha)/(2+\alpha)}$  and  $\kappa_{23} = g/[(1+\alpha)\sqrt{2+\alpha}]$ ; when  $\kappa_{23} = 0$ , there are no physical solutions. The coupling between the two lossy resonators should therefore be nonzero. For a  $PT$ -symmetric trimer, where  $\alpha = 0$ , the EP3 condition becomes  $\kappa_{12} = \kappa_{23} = g/\sqrt{2}$ , which agrees with previous work [16].

Figures 1(b) and 1(c) show the real part and the imaginary part, respectively, of the eigenfrequency evolution at various  $\alpha$  values with respect to  $\kappa_{12}$  when  $\kappa_{13} = 0$  and  $\kappa_{23} = (1+\alpha)^{-3/2}\kappa_{12}$ . Here the gain parameter  $g = 0.1$ . It can be seen that in the weak-coupling regime, when  $\kappa_{12} < \kappa_{EP3}$ , the system has one real eigenvalue and a pair of complex-conjugate eigenvalues, whereas in the strong-coupling regime, when  $\kappa_{12} > \kappa_{EP3}$ , there are three distinct real eigenvalues. The above analysis demonstrates that the proposed system's eigenfrequency characteristics are consistent with those of a pseudo-Hermitian system [18]. The third-order EP, i.e.,  $\kappa_{12} = \kappa_{EP3} = g\sqrt{(1+\alpha)/(2+\alpha)}$ , is the point at which the three eigenvalues coalesce and become degenerate. Moreover, by tuning the scaling factor  $\alpha$ , one can adjust the position of the EP3 to provide additional design flexibility. Even though we consider only the construction of EP3 in a three-dimensional coupled-resonator system, it should be noted that the proposed pseudo-Hermitian system can also be extended to higher-dimensional systems, where HOEPs are envisioned, which is theoretically validated in Supplemental Material [33].

Next, we analyze the perturbation behavior at the third-order EP of the proposed pseudo-Hermitian system, aiming to theoretically validate the enhanced-sensing characteristics. When a capacitive perturbation is introduced on all three resonators, the perturbation Hamiltonian  $\hat{H}_p$  can be written as

$$\hat{H}_p = \frac{1}{2} \begin{pmatrix} \epsilon_1 & 0 & 0 \\ 0 & \epsilon_2 & 0 \\ 0 & 0 & \epsilon_3 \end{pmatrix}. \quad (5)$$

Here, we consider only the case when a capacitive perturbation on the relay resonator is introduced, i.e.,  $\epsilon_1 = \epsilon_3 = 0$  and  $\epsilon_2 = \epsilon$ , where the perturbation parameter  $\epsilon = -\Delta C/(C + \Delta C)$  is related to the capacitive perturbation  $\Delta C$ . For the same value of the gain parameter  $g$ , the frequency response is the most significant when the relay resonator is perturbed. The other two scenarios are discussed and compared in Supplemental Material [33]. By solving for the eigenvalues of the perturbed system with the Hamiltonian  $\hat{H} = \hat{H}_0 + \hat{H}_p$ , we can determine the perturbation behavior of the system at EP3. The characteristic equation  $\det(\hat{H}_0 + \hat{H}_p - \omega\mathbb{I}_3) = 0$  at EP3 when  $\kappa_{13} = 0$  yields

$$\lambda^3 - \frac{\epsilon}{2}\lambda^2 + i\frac{\alpha g}{4(1+\alpha)}\epsilon\lambda - \frac{g^2}{8(1+\alpha)}\epsilon = 0. \quad (6)$$

By expanding the eigenvalues with a Newton-Puiseux series [16]  $\lambda = c_1\epsilon^{1/3} + c_2\epsilon^{2/3} + \dots$  and substituting the series  $\lambda$  into the characteristic equation [Eq. (6)], we have

$$\begin{aligned} c_2^2\epsilon^{7/3} + 2(c_1c_2 - c_2^3)\epsilon^2 + 2(c_1^2/2 - 3c_1c_2^2 - i\beta c_2g)\epsilon^{5/3} \\ - 2(3c_1^2c_2 + i\beta c_1g)\epsilon^{4/3} + (g^2\beta/\alpha - 2c_1^3)\epsilon = 0, \end{aligned} \quad (7)$$

where  $\beta = \alpha/[4(1+\alpha)]$ . Solving the last two terms of Eq. (7), i.e.,  $g^2\beta/2\alpha - c_1^3 = 0$  and  $3c_1c_2 + i\beta g = 0$ , we can obtain the coefficients ( $c_1$  and  $c_2$ ) of the Newton-Puiseux series, which are  $c_1 = (1+\alpha)^{-1/3}g^{2/3}/2$  and  $c_2 = -i\alpha(1+\alpha)^{-2/3}g^{1/3}/6$ . It can be seen that both  $c_1$  and  $c_2$  are decreasing functions of the scaling factor  $\alpha$  for fixed  $g$ . Therefore, as  $\alpha$  increases, the bifurcation of the perturbed eigenvalue will decrease, resulting in a reduction in sensitivity. Thus, in practical use, the loss parameter of the second resonator should be as small as possible. Details of the circumstances under which  $\alpha$  is taken at different values are discussed in Supplemental Material [33]. Here, we consider only the case when  $\alpha = 1$ , i.e., the same loss for the two lossy resonators.

The characteristic equation at EP3 when  $\alpha = 1$  yields  $\lambda^3 - \epsilon\lambda^2/2 + ig\epsilon\lambda/8 - g^2\epsilon/16 = 0$ , from the solving of which the following set of perturbed eigenfrequencies can be obtained:

$$\lambda_1 = (g^2\epsilon/16)^{1/3} - i(g\epsilon^2/4)^{1/3}/6 + \dots, \quad (8a)$$

$$\lambda_2 = (g^2\epsilon/16)^{1/3} e^{i2\pi/3} - i(g\epsilon^2/4)^{1/3} e^{-i2\pi/3}/6 + \dots, \quad (8b)$$

$$\lambda_3 = (g^2\epsilon/16)^{1/3} e^{-i2\pi/3} - i(g\epsilon^2/4)^{1/3} e^{i2\pi/3}/6 + \dots. \quad (8c)$$

The real part and the imaginary part of the perturbed eigenvalues [Eq. (8)] when  $g = 0.1$  are plotted in Figs. 2(a) and 2(b), respectively.

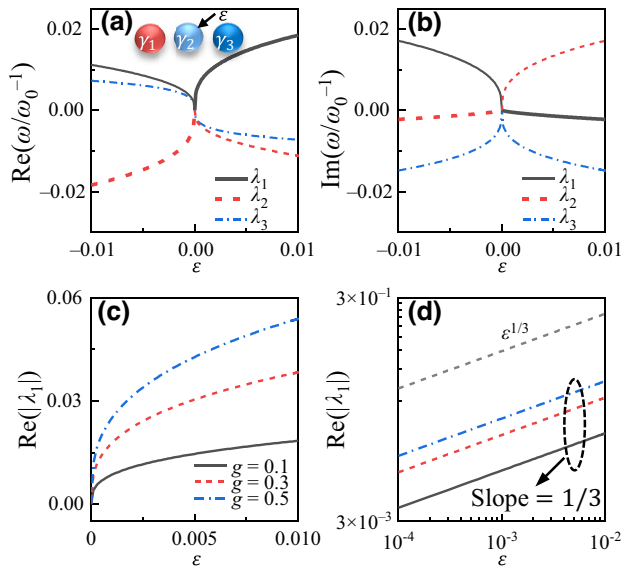


FIG. 2. Theoretical result for (a) the real part and (b) the imaginary part of the perturbed eigenfrequencies around EP3 when  $g = 0.1$ . (c) Bifurcation behavior of  $\lambda_1$  at different  $g$  values when  $\epsilon \in (0, 0.01)$  and (d) the corresponding logarithmic behavior of each curve.

As shown in Fig. 2, the eigenfrequencies bifurcate from a single point at EP3 to three different complex numbers when the perturbation is applied. Moreover, the frequency response follows a cube-root dependence on the capacitive perturbation, which is consistent with the perturbation behavior of a third-order EP. It can be confirmed by the logarithmic behavior in Fig. 2(d), which shows a straight black line with a slope of 1/3. The  $Q$  factor of a resonator circuit, which reflects the sharpness of the dip of the measured reflection-spectrum curve, can be defined on the basis of the complex frequency, i.e.,  $Q = \text{Re}(\omega)/2\text{Im}(\omega)$  [34], indicating that a smaller imaginary part of the eigenfrequency results in a larger  $Q$  factor and thus higher spectral resolution. As shown in Fig. 2(b), one of the three eigenfrequencies exhibits an imaginary part that approaches zero; the corresponding curves are highlighted for clarity, i.e., the dashed red line  $\lambda_2$  when  $\epsilon < 0$  and the solid black line  $\lambda_1$  when  $\epsilon > 0$ . In consequence, the measured reflection spectrum will contain only a single, distinct, narrow and sharp dip. Furthermore, the above-mentioned modes are real only when  $\epsilon = 0$ . Apart from that, the imaginary part has a small absolute value, indicating that the reflection spectrum is sharpest at EP3, but the sharpness will degrade as  $\epsilon$  increases. The other two eigenfrequencies exhibit a greater imaginary part. Therefore, the corresponding reflection dips will be broad and difficult to distinguish, making it difficult to extract the dip frequencies precisely. However, this will not impact the effectiveness of EP3-based sensing, as only the frequencies of the most-pronounced dips are required. We also compare the eigenfrequency response at different

values of the gain parameter in Fig. 2(c), as it can be seen from Eq. (8) that the bifurcation is dependent on the gain parameter  $g$ . The logarithmic behavior in each case is illustrated in Fig. 2(d), together with the dashed gray curve  $\epsilon^{1/3}$  as a reference. It is shown that the cube-root dependence on the perturbation remains the same for different  $g$  values, but the significance of the eigenfrequency bifurcation increases as  $g$  increases. The value of the gain is related to the coupling condition, as has been analyzed. Specifically, the larger the gain, the larger the coupling coefficients  $\kappa_{12}$  and  $\kappa_{23}$ , which is undesirable in real-life applications since it limits the interrogation distance of the sensor and reader circuit. During the experiment, stronger coupling will inevitably introduce coupling between non-adjacent resonators, thereby rendering the conditions for EP3 unsatisfactory. Moreover, strong coupling will make the theoretical result inaccurate since coupled-mode theory is based on a weak-coupling approximation. For a proper coupling condition and to achieve a balance between the sensitivity and usability of the proposed system, the gain parameter is set to 0.1 in the theoretical analysis and subsequent experimental verification.

A printed-circuit-board-based prototype of the pseudo-Hermitian sensing system is constructed for experimental validation. The experimental setup is depicted in the inset in Fig. 4. Printed spiral planar inductors with inductances  $L = 0.847 \mu\text{H}$  are manufactured on three printed-circuit-boards that are coaxially aligned, and the adjacent vertical distances are adjusted with a positioning stage for coupling-parameter tuning (for more information on the coil design, see Ref. [27]). Resonator I is connected to Keysight E5063A VNA to measure the reflection spectrum  $S_{11}$ . Since the VNA itself is a microwave source with an intrinsic impedance  $Z_0$  of  $50 \Omega$ , it is analogous to a negative resistor whose value equals  $Z_0$ . Therefore, resonator I and the VNA constitute a gain resonator with negative resistance if  $R_1$  is less than  $50 \Omega$ . With the preset value  $g = 0.1$  and  $\alpha = 1$ , the coupling condition at EP3 can be calculated as  $\kappa_{12} = 0.0816$  and  $\kappa_{23} = 0.0289$ . We use a  $2.5\text{-}\Omega$  resistor in the relay resonator to match the Ohmic loss of a practical sensor. The circuit parameters are then  $R_2 = R_3 = R = 2.5 \Omega$  and  $R_1 = Z_0 - 2R = 45 \Omega$ , and a variable capacitor is used to mimic a capacitive sensor. The capacitance  $C_{\text{EP3}} = 338.8 \text{ pF}$  at EP3, calculated according to the relation  $g = R_1 \sqrt{C_{\text{EP3}}/L}$ , determines the preset capacitance of the three  $LC$  resonators. A flowchart of the procedure for determining the system parameters is provided as a reference in Supplemental Material [33]. When the perturbation parameter changes from  $-0.01$  to  $0.01$ , the relay resonator's capacitance changes from  $342.22$  to  $335.446 \text{ pF}$ . The experimental results are shown in Fig. 3.

Figures 3(a) and 3(b) show the measured reflection spectra of the conventional readout scheme and the proposed pseudo-Hermitian readout scheme as the capacitive perturbation varies. The theoretical  $S_{11}$  is calculated with

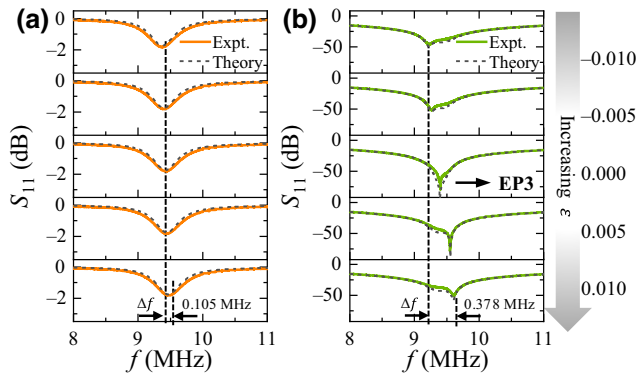


FIG. 3. Experimentally measured reflection spectra (solid curve) of (a) the conventional system when  $\kappa = 0.1$  and (b) the pseudo-Hermitian system around EP3 when  $\kappa_{12} = 0.0816$  and  $\kappa_{23} = 0.0289$  in comparison with the theoretical result (dashed curve) as the capacitive perturbation  $\epsilon$  varies from  $-0.01$  to  $0.01$ . The gain parameter  $g = 0.1$ .

the formula  $S_{11} = 20 \log_{10} |(Z_{in} - Z_0)/(Z_{in} + Z_0)|$ , where  $Z_{in}$  is the input impedance from the terminal of the VNA. The theoretical derivation of the reflection coefficient of both the conventional system and the proposed system is provided in Supplemental Material [33]. Figure 3(a) demonstrates that the dip of the reflection spectra for the conventional readout scheme is shallow, in which case the minimum of the  $S_{11}$  curve exceeds  $-2$  dB. In contrast, the reflection dip is much deeper for the proposed system, and the minimum of  $S_{11}$  can reach several tens of decibels. Consequently, the proposed system has greater spectral resolution than the conventional scheme. Furthermore, Fig. 3(b) demonstrates that the resolution of the spectral dip is greatest at EP3 but degrades as the perturbation increases due to the existence of an imaginary part when  $\epsilon \neq 0$  [see Fig. 2(b)]. As the perturbation increases, so does the value of the imaginary part, leading to a reduction in the  $Q$  factor and thus a loss of spectral resolution. Moreover, the resolution is greater for positive perturbation ( $\Delta C < 0$ ) than for negative perturbation ( $\Delta C > 0$ ),

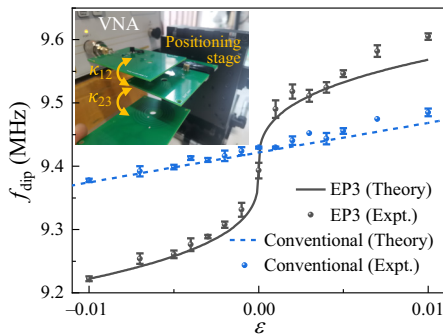


FIG. 4. Comparison of theoretical (curves) and experimental (markers) results for conventional and EP3 sensing schemes. The inset shows the experimental setup for the proposed pseudo-Hermitian sensing system.

indicating an asymmetric  $Q$  factor under symmetric perturbation. This asymmetry phenomenon originates primarily from the approximation in coupled-mode theory. It should also be noted that the experimental  $S_{11}$  spectrum curve at EP3 is not as smooth as the theoretical curve due to the superposition of a noise signal, which is primarily the thermal noise of the circuit [35].

Regarding the sensitivity, as shown in Fig. 4, the eigenfrequency evolution in response to the perturbation parameter at EP3 follows a cube-root dependency on the capacitive perturbation. Compared with the conventional scheme, where a linear dependency is observed, the sensitivity of the proposed pseudo-Hermitian-EP3-based readout scheme is significantly enhanced. In the experiment, for the same sensor capacitance change  $\Delta C = 6.776$  pF, the dip-frequency change for the proposed system is  $0.378$  MHz, while it is only  $0.105$  MHz for the conventional scheme. Moreover, the sensitivity increase is higher as  $\epsilon$  approaches zero.

In summary, we propose a more-general pseudo-Hermitian system based on a radio-frequency circuit that can realize third-order EP under an asymmetric adjacent coupling condition and arbitrary loss parameters. A prototype is built to demonstrate the theoretical proposal experimentally. A cube-root dependency on the perturbation for the perturbed eigenfrequencies is observed when capacitive perturbation is introduced on resonator II (relay resonator), showing a more-significant response than for perturbation of resonators I and III. The sensitivity of the proposed system is much higher than that of the conventional wireless readout method, with the greatest sensitivity increase appearing at EP3. Compared with the conventional wireless sensing system, the proposed circuit shows increased resolution of the measured reflection spectrum. Our work demonstrates that HOEP-enhanced sensing can be used under asymmetric gain-loss distribution, given that the pseudo-Hermitian condition is satisfied, showing potential applications in scenarios such as wireless intraocular pressure monitoring and parameter detection in harsh environments.

*Acknowledgments.*—T.D. is grateful to the National Natural Science Foundation of China for funding under Grant No. 51977165.

- [1] M.-A. Miri and A. Alù, Exceptional points in optics and photonics, *Science* **363**, eaar7709 (2019).
- [2] A. Guo, G. J. Salamo, D. Duchesne, R. Morandotti, M. Volatier-Ravat, V. Aimez, G. A. Siviloglou, and D. N. Christodoulides, Observation of PT-Symmetry Breaking in Complex Optical Potentials, *Phys. Rev. Lett.* **103**, 093902 (2009).
- [3] J. Doppler, A. A. Mailybaev, J. Böhm, U. Kuhl, A. Girschik, F. Libisch, T. J. Milburn, P. Rabl, N. Moiseyev, and S. Rotter, Dynamically encircling an exceptional

- point for asymmetric mode switching, *Nature* **537**, 76 (2016).
- [4] L. Chang, X. Jiang, S. Hua, C. Yang, J. Wen, L. Jiang, G. Li, G. Wang, and M. Xiao, Parity-time symmetry and variable optical isolation in active-passive-coupled microresonators, *Nat. Photon.* **8**, 524 (2014).
- [5] D. Zhang, X.-Q. Luo, Y.-P. Wang, T.-F. Li, and J. You, Observation of the exceptional point in cavity magnon-polaritons, *Nat. Commun.* **8**, 1368 (2017).
- [6] J. Schindler, Z. Lin, J. Lee, H. Ramezani, F. M. Ellis, and T. Kottos, PT-symmetric electronics, *J. Phys. A Math. Theor.* **45**, 444029 (2012).
- [7] B.-B. Zhou, L.-F. Wang, L. Dong, and Q.-A. Huang, Observation of the perturbed eigenvalues of PT-symmetric LC resonator systems, *J. Phys. Commun.* **5**, 045010 (2021).
- [8] C. Zeng, Y. Sun, G. Li, Y. Li, H. Jiang, Y. Yang, and H. Chen, Enhanced sensitivity at high-order exceptional points in a passive wireless sensing system, *Opt. Express* **27**, 27562 (2019).
- [9] Z. Dong, Z. Li, F. Yang, C.-W. Qiu, and J. S. Ho, Sensitive readout of implantable microsensors using a wireless system locked to an exceptional point, *Nat. Electron.* **2**, 335 (2019).
- [10] K. Yin, Y. Huang, C. Ma, X. Hao, X. Gao, X. Ma, and T. Dong, Wireless real-time capacitance readout based on perturbed nonlinear parity-time symmetry, *Appl. Phys. Lett.* **120**, 194101 (2022).
- [11] M. Sakhdari, M. Hajizadegan, Q. Zhong, D. N. Christodoulides, R. El-Ganainy, and P.-Y. Chen, Experimental Observation of PT Symmetry Breaking near Divergent Exceptional Points, *Phys. Rev. Lett.* **123**, 193901 (2019).
- [12] M. Sakhdari, Z. Ye, M. Farhat, and P.-Y. Chen, Generalized theory of PT-symmetric radio-frequency systems with divergent exceptional points, *IEEE Trans. Antennas Propag.* **70**, 9396 (2022).
- [13] M. Sakhdari, M. Hajizadegan, and P.-Y. Chen, Robust extended-range wireless power transfer using a higher-order PT-symmetric platform, *Phys. Rev. Res.* **2**, 013152 (2020).
- [14] H. Hodaei, M.-A. Miri, M. Heinrich, D. N. Christodoulides, and M. Khajavikhan, Parity-time-symmetric microring lasers, *Science* **346**, 975 (2014).
- [15] L. Feng, Z. J. Wong, R.-M. Ma, Y. Wang, and X. Zhang, Single-mode laser by parity-time symmetry breaking, *Science* **346**, 972 (2014).
- [16] H. Hodaei, A. U. Hassan, S. Wittek, H. Garcia-Gracia, R. El-Ganainy, D. N. Christodoulides, and M. Khajavikhan, Enhanced sensitivity at higher-order exceptional points, *Nature* **548**, 187 (2017).
- [17] J. Wiersig, Enhancing the Sensitivity of Frequency and Energy Splitting Detection by Using Exceptional Points: Application to Microcavity Sensors for Single-Particle Detection, *Phys. Rev. Lett.* **112**, 203901 (2014).
- [18] A. Mostafazadeh, Pseudo-Hermiticity versus PT symmetry: The necessary condition for the reality of the spectrum of a non-Hermitian Hamiltonian, *J. Math. Phys.* **43**, 205 (2002).
- [19] X. Hao, K. Yin, J. Zou, R. Wang, Y. Huang, X. Ma, and T. Dong, Frequency-Stable Robust Wireless Power Transfer Based on High-Order Pseudo-Hermitian Physics, *Phys. Rev. Lett.* **130**, 077202 (2023).
- [20] W. Xiong, Z. Li, Y. Song, J. Chen, G.-Q. Zhang, and M. Wang, Higher-order exceptional point in a pseudo-Hermitian cavity optomechanical system, *Phys. Rev. A* **104**, 063508 (2021).
- [21] C. C. Collins, Miniature passive pressure transducer for implanting in the eye, *IEEE Trans. Biomed. Eng. BME-14*, 74 (1967).
- [22] P.-J. Chen, D. C. Rodger, S. Saati, M. S. Humayun, and Y.-C. Tai, Microfabricated implantable parylene-based wireless passive intraocular pressure sensors, *J. Microelectromech. Syst.* **17**, 1342 (2008).
- [23] P.-J. Chen, S. Saati, R. Varma, M. S. Humayun, and Y.-C. Tai, Wireless intraocular pressure sensing using microfabricated minimally invasive flexible-coiled LC sensor implant, *J. Microelectromech. Syst.* **19**, 721 (2010).
- [24] N. Xue, S.-P. Chang, and J.-B. Lee, A SU-8-based microfabricated implantable inductively coupled passive RF wireless intraocular pressure sensor, *J. Microelectromech. Syst.* **21**, 1338 (2012).
- [25] P.-Y. Chen, M. Sakhdari, M. Hajizadegan, Q. Cui, M. M.-C. Cheng, R. El-Ganainy, and A. Alù, Generalized parity-time symmetry condition for enhanced sensor telemetry, *Nat. Electron.* **1**, 297 (2018).
- [26] M. Yang, Z. Ye, M. Farhat, and P.-Y. Chen, Ultrarobust wireless interrogation for sensors and transducers: A non-Hermitian telemetry technique, *IEEE Trans. Instrum. Meas.* **70**, 1 (2021).
- [27] K. Yin, Y. Huang, W. Yin, X. Hao, X. Ma, and T. Dong, Ultrahigh-Resolution Wireless Capacitance Readout Based on a Single Real Mode in a Perturbed PT-Symmetric Electronic Trimer Sandwich, *Phys. Rev. Appl.* **18**, 064020 (2022).
- [28] B.-B. Zhou, W.-J. Deng, L.-F. Wang, L. Dong, and Q.-A. Huang, Enhancing the Remote Distance of LC Passive Wireless Sensors by Parity-Time Symmetry Breaking, *Phys. Rev. Appl.* **13**, 064022 (2020).
- [29] C. Zeng, K. Zhu, Y. Sun, G. Li, Z. Guo, J. Jiang, Y. Li, H. Jiang, Y. Yang, and H. Chen, Ultra-sensitive passive wireless sensor exploiting high-order exceptional point for weakly coupling detection, *New J. Phys.* **23**, 063008 (2021).
- [30] Y. Jia, K. Sun, F. J. Agosto, and M. T. Quinones, Design and characterization of a passive wireless strain sensor, *Meas. Sci. Technol.* **17**, 2869 (2006).
- [31] P. Yeon, M.-g. Kim, O. Brand, and M. Ghoovanloo, Optimal design of passive resonating wireless sensors for wearable and implantable devices, *IEEE Sens. J.* **19**, 7460 (2019).
- [32] S. Assawaworrarit, X. Yu, and S. Fan, Robust wireless power transfer using a nonlinear parity-time-symmetric circuit, *Nature* **546**, 387 (2017).
- [33] See Supplemental Material at <http://link.aps.org/supplemental/10.1103/PhysRevApplied.20.L021003> for a generalized theoretical framework, a comparison of system perturbation behavior in different scenarios, and the derivation of the reflection coefficient.
- [34] D. M. Pozar, *Microwave Engineering* (John Wiley & Sons, New York, NY, USA, 2011).
- [35] Z. Xiao, H. Li, T. Kottos, and A. Alù, Enhanced Sensing and Nondegraded Thermal Noise Performance Based on PT-Symmetric Electronic Circuits with a Sixth-Order Exceptional Point, *Phys. Rev. Lett.* **123**, 213901 (2019).